Developmental Biology **242,** 161–173 (2002)
doi:10.1006/dbio.2001.0543, available online at http://www.idealibrary.com on IDEAL®

The *UCU1 Arabidopsis* Gene Encodes a SHAGGY/GSK3-like Kinase Required for Cell Expansion along the Proximodistal Axis

José Manuel Pérez-Pérez, María Rosa Ponce, and José Luis Micol[1]

División de Genética and Instituto de Bioingeniería, Universidad Miguel Hernández, Campus de Elche, 03202 Elche, Alicante, Spain

Most signal transduction pathways central to development are not shared by plants and animals. Such is the case of the Wingless/Wnt signaling pathway, whose components play key roles in metazoan pattern formation and tumorigenesis, but are absent in plants, with the exception of SHAGGY/GSK3, a cytoplasmic protein kinase represented in the genome of *Arabidopsis thaliana* by a family of 10 *AtSK* genes for which mutational evidence is scarce. Here, we describe the characterization of mutant alleles of the *Arabidopsis ULTRACURVATA1* (*UCU1*) gene, the two strongest of which dramatically reduce cell expansion along the proximodistal axis, dwarfing the mutant plants, whose cells expand properly across but not along most organs. Proximodistal expansion of adaxial (dorsal) and abaxial (ventral) leaf cells exhibits a differential dependence on UCU1 function, as suggested by the leaves of *ucu1* mutants, which are rolled spirally downward in a circinate manner. We have positionally cloned the *UCU1* gene, which encodes an AtSK protein involved in the cross-talk between auxin and brassinosteroid signaling pathways, as indicated by the responses of *ucu1* mutants to plant hormones and the phenotypes of double mutants involving *ucu1* alleles.

***Key Words: Arabidopsis*; plant leaf development; *ultracurvata* mutants; brassinosteroid signaling; SHAGGY/GSK3-like kinases.**

INTRODUCTION

A plethora of genetic and molecular studies support the notion that plant development has evolved its own signal transduction pathways (McCarty and Chory, 2000), an idea reinforced by the comparative genome analysis between *Arabidopsis thaliana*, *Caenorhabditis elegans*, and *Drosophila melanogaster*. Indeed, most components of the developmental signaling pathways common to animals, such as Wingless/Wnt, Hedgehog, Notch/lin12, JAK/STAT, TGF-β/SMADs, receptor tyrosine kinase/Ras, or the nuclear steroid hormone receptors, are absent in *A. thaliana* (McCarty and Chory, 2000; The *Arabidopsis* Initiative, 2000; Wigge and Weigel, 2001). One of the few known exceptions is a family of 10 genes found in the genome of *A. thaliana* (Dornelas *et al.*, 1998), which code for proteins that share a highly conserved catalytic protein kinase domain about 70% identical to those of SHAGGY (SGG) of *D. melanogaster* (Siegfried *et al.*, 1990) and mammalian glycogen synthase kinase-3 (GSK3; Woodgett, 1990). SGG/GSK3 kinases have been described in many animal species, where they are known to be involved in developmental processes such as specification of embryonic axes, segment polarity, cell fate determination, and tumorigenesis (Ferkey and Kimelman, 2000; Kim and Kimmel, 2000). In these systems, the SGG/GSK3 kinase is involved in the transduction of the Wingless/Wnt signal to the nucleus.

There is a dearth of functional and mutational information for the *SGG/GSK3-like* genes of *A. thaliana*, which have been named *AtSK* (formerly designated *ASK*) genes (Dornelas *et al.*, 1998, 1999, 2000). Whereas some *AtSK* genes are preferentially transcribed in developing pollen (Tichtinsky *et al.*, 1998), specific regions of flower organ primordia (Dornelas *et al.*, 2000), or the suspensor cells of the embryo (Dornelas *et al.*, 1999), others are ubiquitously expressed in aerial organs (Dornelas *et al.*, 1999). Another member of this family, *AtGSK1*, is induced by NaCl and abscisic acid (Piao *et al.*, 1999). Plants transgenic for antisense constructs of *AtSK11* (*AtSKα*) or *AtSK12* (*ASKγ*)

[1] To whom correspondence should be addressed. Fax: 34 96 665 85 11. E-mail: jlmicol@umh.es.

0012-1606/02 $35.00

TABLE 1
Novel SSLP Primer Sets Used in This Work

Marker	BAC	Position in BAC	Oligonucleotide sequences (5′→3′)		PCR product size (bp)	
			Fluorescently labeled forward primer	Unlabeled reverse primer	L*er*	Col-0
AtFCA9.1	FCA9	14931-15182	ACTGCATCTCTAGTAATAAAAGG[a]	GCAAATGAACCAAACCCACTG	246	252
AtT6K21.1	T6K21	53045-53234	ACGAATGCCGAGAAAATAGACG[a]	CTAACTAGATCGTCCCTCGTC	139	191
AtF28J12.3	F28J12	68473-68736	AAATCTCAGATCCGTCATTTCCA[b]	CCTTTATCAATGGATGAGGAATC	257	265
AtF28A21.2	F28A21	10634-10984	CTGGAATACATGTTGAAATGCAC[b]	CAATTGCCGGTTCGAATCCTAAG	354	352
AtF28A21.1	F28A21	55146-55363	GAAGAGCTGGATTCACATGG[a]	AACACAAGCAGCTTTACCTTAT	224	219
AtF28A21.3	F28A21	70578-70782	GACAATGGACTGCTGAAGAAG[c]	CCATTTACGCAATCCATACTTC	216	207

Each primer pair included one oligonucleotide labeled with 6-FAM (6-carboxyfluorescein),[a] HEX (4, 7, 2′, 4′, 5′, 7′-Hexachloro-6-carboxyfluorescein),[b] or TET (4, 7, 2′, 7′-Tetrachloro-6-carboxyfluorescein)[c] phosphoramidites.

display defects in the number of floral organs, primarily due to an increase in meristem size (Dornelas *et al.*, 2000). Thus, our understanding of the function in plants of these evolutionary ancient proteins is lacking.

Although the leaf is the main photosynthetic plant organ, the question of how plant leaves develop is far from being answered at the genetic level (Byrne *et al.*, 2001; Poethig, 1997; Scanlon, 2000; Sinha *et al.*, 1993; Tsiantis and Langdale, 1998). Aiming to contribute to a better understanding of leaf ontogeny, we have followed three complementary genetic approaches in the model plant *A. thaliana*: the study of natural variations in leaf architecture among wild-type races (Candela *et al.*, 1999; J. M. P-P., J. Serrano-Cartagena, and J. L. M., submitted), the analysis of leaf mutants obtained by previous authors (Serrano-Cartagena *et al.*, 1999, 2000), and the isolation of new leaf mutants (Berná *et al.*, 1999; Robles and Micol, 2001). Here, we present the genetic and molecular analysis of three mutants that carry alleles of the *ULTRACURVATA1* (*UCU1*) gene, whose leaves are rolled spirally downward in a circinate manner. The two strongest *ucu1* alleles cause brassinosteroid insensitivity and dwarfism, which is due to a severe reduction in cell expansion along the proximodistal axis. The *UCU1* gene was cloned by a map-based approach and found to encode a conserved SGG/GSK3-like kinase. The responses of *ucu1* mutants to exogenous plant hormones and the genetic analyses of double mutants involving *ucu1* alleles indicate that *UCU1* is a key component of several signaling pathways controlling cell expansion and overall plant growth, including those of auxins and brassinosteroids.

MATERIALS AND METHODS

Plant Materials, Growth Conditions, and Crosses

A. thaliana (L.) Heyhn. Landsberg *erecta* (L*er*) and Columbia-0 (Col-0) ecotypes and the N379 mutant line (carrying the *shy2–3* allele) were supplied by the Nottingham *Arabidopsis* Stock Centre. The *ucu1* mutants were isolated after EMS mutagenesis in our laboratory (Berná *et al.*, 1999). Following the nomenclature rules of Meinke and Koornneef (1997), the phenotype of the mutants studied in this work is referred to as Ultracurvata1 (Ucu1), with the first letter capitalized. The wild-type allele is designated as *ULTRACURVATA1* (*UCU1*), in capital letters, and mutant alleles as *ultracurvata1* (*ucu1-1*, *ucu1-2*, and *ucu1-3*), in italic lowercase letters, irrespective of being recessive or semidominant. The protein product of the *UCU1* gene is denoted as UCU1, in capital letters without italics.

The CS3151 tetraploid line and the *BRI1/bri1-1* (CS3723), *DIM1/dim1-1* (CS8100), *det2-1/det2-1* (CS6159), *ga5-1/ga5-1* (CS62), and *axr2-1/axr2-1* (CS3077) mutants were supplied by the *Arabidopsis* Biological Resource Centre. Cultures were performed as described in Ponce *et al.* (1998), at 20 ± 1°C and 60–70% relative humidity under continuous illumination of 7000 lx. Crosses were performed as described in Berná *et al.* (1999).

With the aim to obtain triploid F_1 plants, five crosses were made between homozygous *ucu1* mutants (in a L*er* genetic background) and the CS3151 tetraploid line (in a Col-1 genetic background). In order to confirm the triploid nature of the F_1 progeny, microsatellite polymorphisms between L*er* and Col-1 were tested as previously described (Ponce *et al.*, 1999), using a high-throughput genotyping procedure based on the simultaneous coamplification by PCR of 21 polymorphic microsatellites and the fluorescent semiautomated detection and sizing of the products. At least three F_1 plants from each cross were tested, all of which were shown to carry both the L*er* and Col-1 microsatellite alleles.

Photomicrography and Morphometric Analysis

Root and hypocotyl lengths were determined in seedlings grown on vertically oriented agar plates. Dry weight was measured in plants oven-dried for 2 days at 60°C. Leaves from the third node were excised, treated with chloral hydrate, mounted on slides, and camera lucida drawn for morphometric analysis as described in Candela *et al.* (1999). All the siliques from the 4th to the 15th from at least 5 plants were scored for each genotype.

A Leica DMRB microscope was used for photomicrography and camera lucida drawing. Rosette pictures were taken in a Leica MZ6 stereomicroscope equipped with a Leica MPS48 photomicrography system. Image analysis was performed by using the NIH Image program (available at http://rsb.info.nih.gov/nih-image/). Third

TABLE 2
Novel SNP Primer Sets Used in This Work

Marker	Position in BAC	Oligonucleotide sequences (5′→3′)		Polymorphisms between Col-0 and L*er*[a]
		Forward primer	Reverse primer	
At4g18640	21606-22636	GAACGGCTTACTGTCT	ATACAAACACATATCGAA	21739(A→G); 21745(Del21745-21767); 21843(G→A);
		TCAACA	ACTCGT	21847(T→A); 21849(T→C); 21851(G→C); 21879(A→C); 21952(A→T); 22021(G→A); 22033(C→A); 22039(T→C); 22096(Del22096-22097); 22123(Del22123); 22144(C→T); 22158(C→A); 22171(A→G); 22249(G→A); 22328(G→T)
At4g18670	36210-37503	TGATCTCTGCGCAGGT	ATGAATAGGGCTGAGCT	36292(G→C); 36326(A→G); 36346(G→C); 36357(C→G);
		CTCG	GTGC	36363(A→C); 36468(T→A); 36492(C→A); 36540(A→C); 36542-36543(GA→AG); 36597(C→T); 36603(A→G); 36636(C→T); 36669(A→G); 36941(C→A); 36960(T→C); 36966(G→C); 37342(G→A); 37352(C→A)
At4g18700	48645-49899	GATTCGTCTCCAAAAG	CATTGCAACCCATTTTGT	48715(C→T); 48766(C→T); 48768(A→G); 48886(C→A);
		CTTCGA	TAGTC	49201(T→A); 49204(A→C); 49261(C→T); 49455(G→C); 49565(A→G); 49704(C→G); 49732(G→C); 49788(T→A); 49813(A→C)
At4g18740	62304-63420	AAAATGTTTCAGCTTTA	TGTTGTGAGGTGAAGAA	62544(T→C); 62705(A→G); 62740(Del62740-62741);
		CAAGAATG	AGAGG	62964(C→T); 63019(T→A); 63021(T→A); 63170(Del63170-63171)

[a] Numbers indicate positions of the polymorphisms found in the F28A21 BAC sequence (which corresponds to a Col-0 background). The Col-0→L*er* base changes are indicated. "Del" denotes a deletion found in the sequence of L*er* as compared to that of Col-0.

node leaves were longitudinally sectioned 21 days after sowing as described in Serrano-Cartagena *et al.* (2000) and photographed halfway along the midvein and the leaf margin. Confocal microscopy sections of fresh leaves were obtained by using a Leica TCS-NT microscope equipped with FITC/TRITC filters.

Physiological Analyses

For gravitropic response analysis, seeds were sown on agar plates that were kept vertically oriented for 7 days and then clockwise rotated 135° for observation 3 days later. Photomorphogenic response was analyzed in seedlings grown in the dark on vertically oriented agar plates. Hypocotyls were drawn for morphometric analysis 11 days after sowing.

For phytohormone treatments, seedlings were transferred 7 days after sowing from nonsupplemented medium to media supplemented with 0.05 or 0.1 μM 24-epibrassinolide (Sigma E1641); 1, 10, or 100 μM gibberellic acid (GA_3; Sigma G1025); 0.01, 0.1, or 1 μM indole-3-acetic acid (IAA; Gibco BRL 11450-012); 0.01 or 0.1 μM 6-benzylaminopurine (BA; Sigma B3408), and pictures were taken 15 days later. Plants treated with GA_3 or 24-epibrassinolide were transferred to soil 24 days after sowing, and they were then sprayed for 2 weeks, at 3-day intervals, with a hormone solution at the same concentration as that already on the plates. To study the effect of brassinosteroids in cell elongation, seedlings were grown in the dark on agar plates supplemented with 0.01, 0.1, or 1 μM 24-epibrassinolide or 0.01 or 0.1 μM 22(S),23(S)-homobrassinolide (Sigma H1267), and observed 11 days after sowing. The effect of abscisic acid (ABA; Sigma A7383) was studied by determining germination rates 15 days after sowing on agar plates supplemented

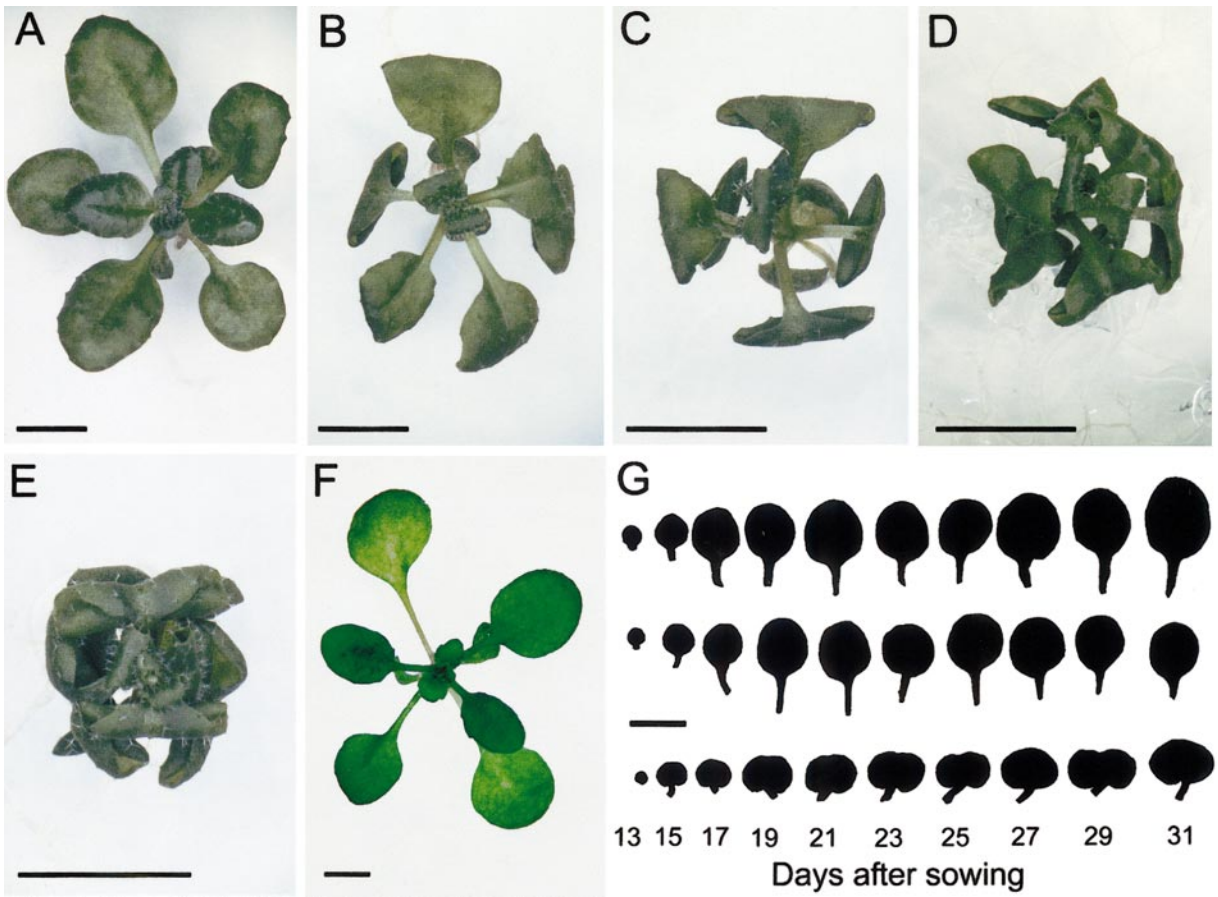

FIG. 1. Phenotype of *ucu1* mutants. (A–F) Rosette phenotypes of the wild type and plants carrying *ucu1* mutant alleles. Rosettes are shown from (A) a L*er* wild-type individual and (B) *ucu1-3/ucu1-3*, (C) *UCU1/ucu1-1*, (D) *ucu1-1/ucu1-3*, and (E) *ucu1-2/ucu1-2* mutant plants. (F) *UCU1/UCU1/ucu1-1* triploid plant. (G) Time course of the expansion of the third vegetative leaf: L*er* (top), *ucu1-3/ucu1-3* (center), and *ucu1-1/ucu1-1* (bottom). Scale bars: 4 (A–F) or 5 mm (G). Pictures (A–F) were taken 21 days after sowing.

with 3 or 5 μM ABA. For root-elongation assays, 30 seedlings of each genotype were grown in vertically oriented agar plates supplemented with 0, 25, 50, 100, 300, or 500 nM 24-epibrassinolide, or 0, 10, 20, or 50 nM 2,4-D (2,4-dichlorophenoxyacetic acid; Gibco BRL 11215-019), and root length was measured for at least 25 seedlings 11 days after sowing.

Positional Cloning of the UCU1 Gene

Low-resolution gene mapping was performed by combining SSLP (Bell and Ecker, 1994) and CAPS (Konieczny and Ausubel, 1993) markers. Since all the mutant lines subjected to linkage analysis in this work derived from the L*er* ecotype, they were first crossed to Col-0, and F_2 phenotypically recessive individuals were collected and their DNA isolated as described in Ponce *et al.* (1999). Novel SSLP and SNP markers developed in this work to positionally clone the *UCU1* gene are described in Tables 1 and 2. Multiplex PCR amplification conditions and automated fragment sizing of amplified microsatellites were as described in Ponce *et al.* (1999). Map distances were determined by using Kosambi's map function (Kosambi, 1944).

Sequencing reactions were carried out with ABI PRISM BigDye Terminator Cycle Sequencing kits according to the instructions of the manufacturer. Electrophoreses were performed on an ABI PRISM 377 DNA Sequencer.

Analysis of Amino Acid Sequences

Members of the SGG/GSK3 family related to UCU1 were identified in the GenBank database (Karsch-Mizrachi and Ouellette, 2001) by using the BLAST algorithm (Altschul *et al.*, 1990). A multiple alignment of the catalytic domain of these kinases, encompassing 285 residues (Hanks, 1991), was obtained by using the CLUSTAL X 1.5b program (Thompson *et al.*, 1997) and shaded with the BOXSHADE 3.21 program (Hofmann and Baron, unpublished; http://www.ch.embnet.org/software/BOX_form.html).

RT-PCR

Transcription of the *UCU1* gene was tested by reverse-transcriptase–PCR (RT-PCR) in RNA isolated from leaves and flower buds as described in Ponce *et al.* (2000) by using the following primer pairs: SH1F (5′-TCTCTATCGCCACAATGATCATT-3′) and SH1R (5′-CGTGAGCAGATGTAAGAAATGTT-3′), or SH3F (5′-ATCTGT-

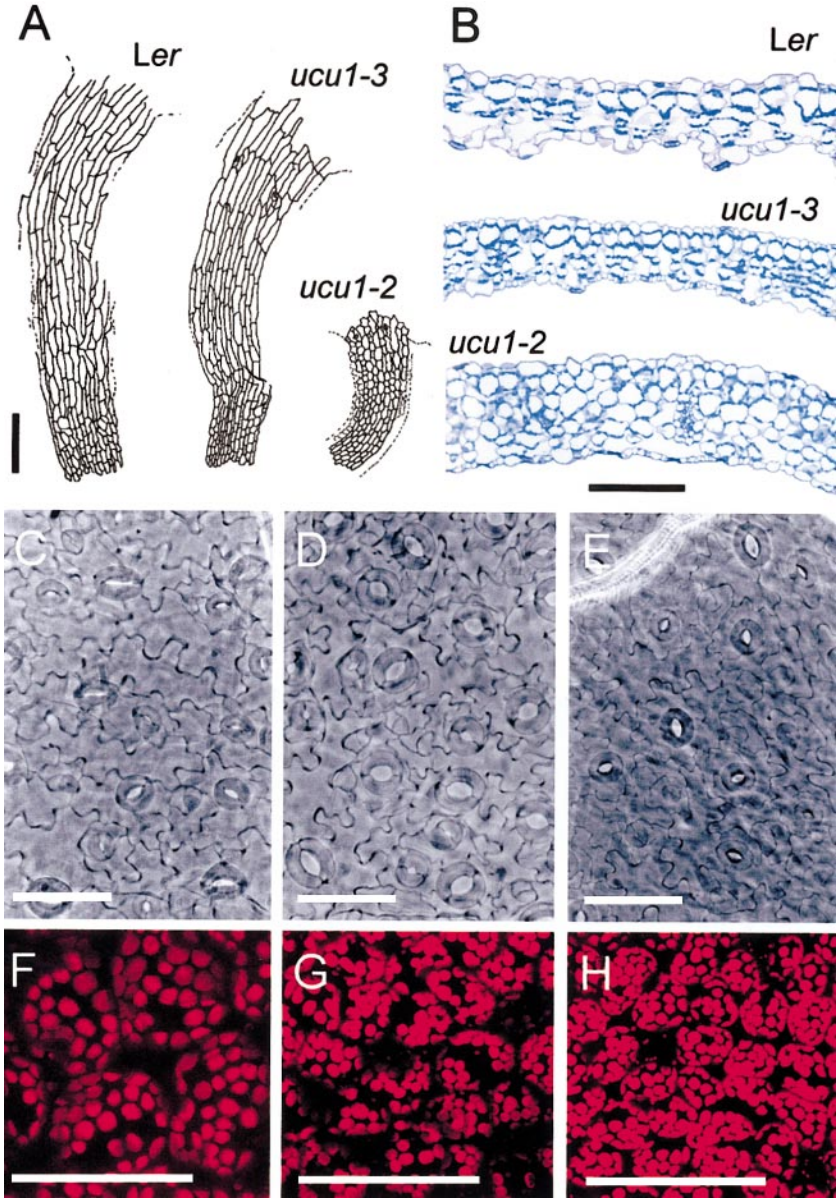

FIG. 2. Ultrastructure of the wild-type L*er* and *ucu1* homozygous mutants. (A) Light microscopy drawings of whole hypocotyls. (B) Longitudinal sections of vegetative leaves. (C–E) Micrographs of the abaxial epidermis and (F–H) confocal microscopy sections of third node vegetative leaves from the wild-type L*er* (C, F) and *ucu1-3* (D, G) or *ucu1-1* (E, H) homozygous plants. Scale bars: 250 (A), 50 (B), or 100 μm (C–H). Samples were collected 11 (A) or 21 (B–H) days after sowing.

GACTTTGGCAGTGCG-3′) and SH5R (5′-AGTATTGAAGCA-GCCTTGATGC-3′).

RESULTS

Genetic Analysis of ultracurvata1 Mutants

In order to analyze leaf development, we sought to identify EMS-induced mutations affecting leaf morphology in *A. thaliana* (Berná *et al.*, 1999; Robles and Micol, 2001). One of the stronger phenotypes found is that of the *ultracurvata* (*ucu*) mutants, whose vegetative and cauline leaves are circinate, rolled spirally downward (Figs. 1B–1E). We obtained three alleles of the *ULTRACURVATA1* (*UCU1*) gene, two of which, *ucu1-1* and *ucu1-2*, are semidominant, their phenotypic effects being indistinguishable and stronger than the recessive *ucu1-3* mutation (Table 3). Homozygous *ucu1* individuals and the hybrid F_1 progeny of their

TABLE 3
Phenotypic Segregations in the Progeny of Crosses Involving *ucu1* Mutations

Cross (♀ × ♂)	F_1	F_2						
		UcuX	UcuS	UcuI	UcuW	WT	χ^2 value	*P*
ucu1-1/ucu1-1 × *ucu1-2/ucu1-2*	37 UcuX	193					—	
ucu1-1/ucu1-1 × *ucu1-3/ucu1-3*	26 UcuS	44	79		39		0.41[a]	0.81
ucu1-2/ucu1-2 × *ucu1-3/ucu1-3*	35 UcuS	40	71		41		0.67[a]	0.72
UCU1/UCU1 × *ucu1-1/ucu1-1*	41 Ucu*I*	58		85		55	4.05[a]	0.13
UCU1/UCU1 × *ucu1-2/ucu1-2*	24 Ucu*I*	83		148		87	1.62[a]	0.44
UCU1/UCU1 × *ucu1-3/ucu1-3*	26 WT				46	154	0.33[b]	0.57
UCU1/UCU1/UCU1/UCU1 × *ucu1-1/ucu1-1*	34 T						—	
UCU1/UCU1/UCU1/UCU1 × *ucu1-2/ucu1-2*	12 T						—	

Note. UcuX, Extreme Ucu leaf phenotype (that of *ucu1-1/ucu1-1*, *ucu1-2/ucu1-2*, and *ucu1-1/ucu1-2* individuals; Fig. 1E). UcuS, Strong Ucu leaf phenotype (*ucu1-1/ucu1-3* and *ucu1-2/ucu1-3*; Fig. 1D). Ucu*I*, Intermediate Ucu leaf phenotype (*UCU1/ucu1-1* and *UCU1/ucu1-2*; Fig. 1C). UcuW, Weak Ucu leaf phenotype (*ucu1-3/ucu1-3*; Fig. 1B). T, Triploid plants with no Ucu phenotypic traits (Fig. 1F); and WT, Wild type (Fig. 1A). The χ^2 values represent the fit of the F_2 data to an expected 1:2:1[a] or 3:1[b] phenotypic segregation.

intercrosses and crosses to the wild type (*UCU1/UCU1*) can be ordered in an ascending series of mutant phenotypic strength as follows: *UCU1/UCU1* = *ucu1-3/UCU1* < *ucu1-3/ucu1-3* < *ucu1-1/UCU1* < *ucu1-1/ucu1-3* < *ucu1-1/ucu1-1* = *ucu1-1/ucu1-2* (Table 3; Figs. 1A–1E). Tetraploid plants in a Col-1 genetic background were crossed to either *ucu1-1/ucu1-1* or *ucu1-2/ucu1-2* mutants in a L*er* background, and no Ucu phenotypic trait was displayed by the F_1 triploid progeny (Table 3; Fig. 1F). Microsatellite polymorphisms between L*er* and Col-1 were tested in the latter plants, which were demonstrated to be *UCU1/UCU1/ucu1*.

Pleiotropy of the Ucu1 Mutant Phenotype

The Ucu1 mutant phenotype is pleiotropic, *ucu1-1/ucu1-1* and *ucu1-2/ucu1-2* individuals being dwarf with hypocotyls, leaf petioles, and roots shorter than those of the wild type, with compact dark green rosettes, reduced inflorescence length with a partial loss of apical dominance, and low fertility (Table 4; Figs. 1B–1E), a phenotype reminiscent of mutants impaired in the synthesis or perception of brassinosteroid hormones (Altmann, 1999). Cell morphology was studied in the *ucu1* mutants, focusing on those organs displaying a reduction in length along the proximodistal axis: the hypocotyl, petioles, siliques, and roots, the latter displaying a higher epidermal hair density than the wild type. Cell numbers were not significantly different compared with the wild type, but cell length was remarkably diminished in those organs. As an illustration, fully expanded epidermal cells of *ucu1-3/ucu1-3* and *ucu1-2/ucu1-2* hypocotyls were respectively 1.5- and 5.5-fold shorter than those of L*er* (Fig. 2A).

Leaf Architecture of ucu1 Mutants

Although similar in width to those of the wild type, vegetative and cauline leaves of *ucu1* mutants show a reduced expansion along the proximodistal axis (Fig. 1G). A reduction in length is suffered by both the lamina and the petiole in *ucu1-1/ucu1-1* and *ucu1-2/ucu1-2* individuals, and principally by the lamina in *UCU1/ucu1-1* and *UCU1/ucu1-2*. Only the apical portion of fully expanded leaves is curled in *ucu1-3/ucu1-3* plants, whose petioles are otherwise apparently normal.

The number of cells along the proximodistal axis was similar in mutant and wild-type leaves. On the contrary, cell size was remarkably reduced in the mutants, a trait that is more pronounced in abaxial (ventral) epidermal cells. In addition, there is an increase in thickness of the

TABLE 4
Body Parameters of the Wild-Type and Homozygous *ucu1* Mutants

	L*er*	*ucu1-3*	*ucu1-1*
Root length[a]	64.3 ± 9.0	40.9 ± 10.5	28.9 ± 12.6
Hypocotyl length[a]	1.9 ± 0.3	1.7 ± 0.3	1.0 ± 0.2
No. of vegetative leaves[b]	9.4 ± 0.6	9.5 ± 0.5	9.5 ± 0.8
Rosette diameter[b]	21.9 ± 4.3	17.7 ± 1.7	7.6 ± 1.7
Fresh weight[b]	24.4 ± 4.0	15.2 ± 3.5	10.7 ± 3.9
Dry weight[b]	1.9 ± 0.4	1.4 ± 0.5	1.0 ± 0.9
Petiole length[b]	4.0 ± 0.9	3.6 ± 0.9	2.0 ± 0.6
Lamina length[b]	7.3 ± 1.0	5.4 ± 0.9	3.1 ± 0.3
Lamina width[b]	5.7 ± 0.9	4.8 ± 0.6	5.4 ± 0.6
Pedicel length[c]	3.5 ± 1.1	1.4 ± 0.3	1.8 ± 0.7
Silique length[c]	8.5 ± 1.0	6.8 ± 0.6	4.6 ± 0.9
Seeds per silique[c]	34.1 ± 5.2	26.7 ± 2.9	15.8 ± 4.1
Primary stem length[c]	197.8 ± 30.9	149.6 ± 17.7	59.9 ± 8.9
No. of secondary stems[c]	2.1 ± 0.7	3.9 ± 0.9	4.4 ± 0.4

Note. Values are means of at least 20 measurements ± standard deviation. Lengths are indicated in mm, weights in mg. Measurements were taken from plant material collected 11,[a] 21,[b] or 49[c] days after sowing (see Materials and Methods).

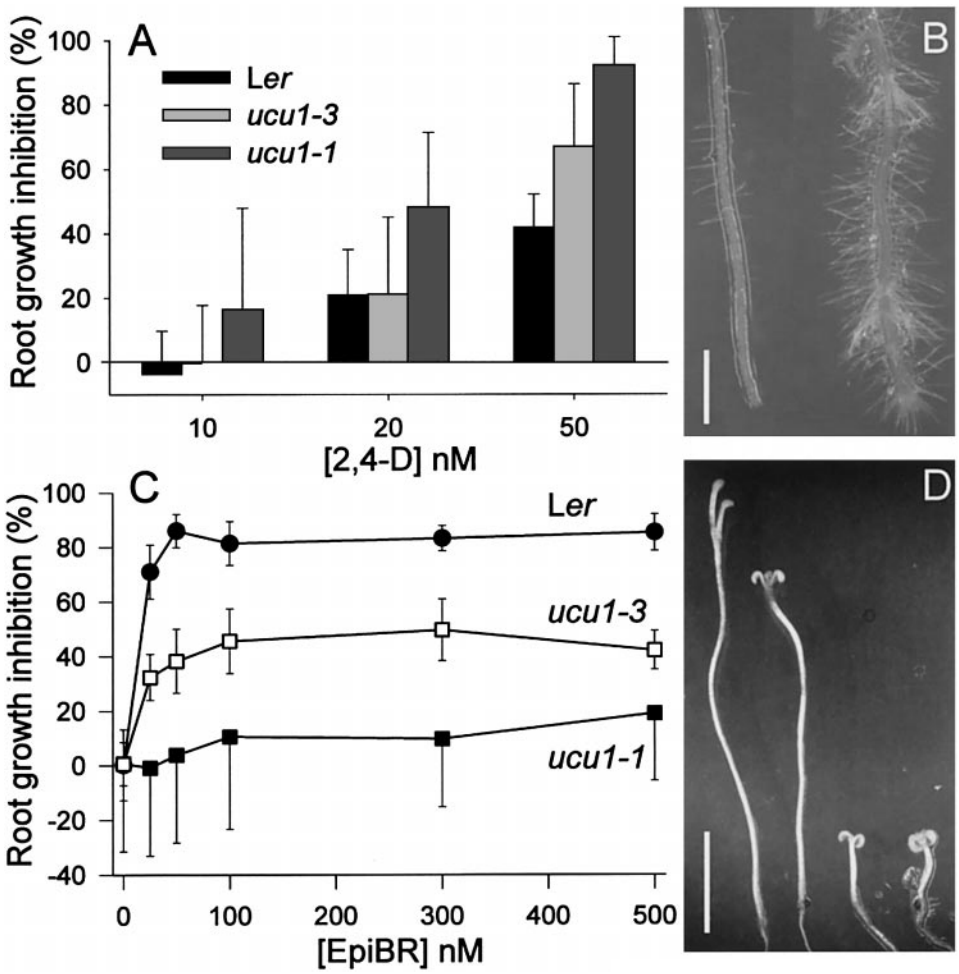

FIG. 3. Physiological analyses of the *ucu1* mutants. (A) Growth response of *ucu1* mutants to the synthetic auxin 2,4-D. (B) Root phenotype of L*er* (left) and *ucu1-1/ucu1-1* (right) seedlings when grown on media supplemented with 20 nM 2,4-D. (C) Root growth inhibition by 24-epibrassinolide. (D) De-etiolated phenotype of *ucu1* homozygous mutants. From left to right, wild-type L*er* and *ucu1-3*, *ucu1-2*, and *ucu1-1* mutants. Each point in (A) and (C) represents mean data ($n > 25$) of the reduction in root length displayed by L*er* and *ucu1/ucu1* plants grown on phytohormone supplemented media, referred to that of the controls grown on nonsupplemented media. Seedlings were analyzed 11 days after sowing, those shown in (D) grown in the dark. Scale bars: 2 mm (B, D).

ucu1-1 and *ucu1-2* mutant leaves (Fig. 2B). Hence, cell expansion is also impaired in *ucu1* leaves, whose circinate phenotype was shown to be associated with an extreme misexpansion of abaxial epidermal cells (Figs. 2D and 2E), a result that indicates a differential requirement for UCU1 function by adaxial (dorsal) and abaxial leaf cells. The leaves of *ucu1-1* and *ucu1-2* mutants are dark green, probably as a consequence of both the dense arrangement of chloroplasts observed in confocal microscopy sections (Figs. 2G and 2H) and the increased number of inner cell layers.

Physiological Analyses of the ucu1 Mutants

Growth of the *ucu1* mutants in the presence of different plant hormones was tested (see Materials and Methods), and in no case was the mutant phenotype rescued to the wild-type by an exogenous hormone. Growth responses of the *ucu1* mutants to cytokinin, giberellin, abscisic acid, and the naturally occurring auxin indole-3-acetic acid (IAA) were similar to that of the wild type. On the contrary, severe root growth inhibition (Fig. 3A) and undifferentiate growth were observed in these mutants when grown at low concentrations of the synthetic auxin 2,4-dichlorophenoxyacetic acid (2,4-D) which do not affect wild-type roots (Fig. 3B). Moreover, the roots of *ucu1* mutants elongated in the presence of 24-epibrassinolide concentrations that completely inhibit wild-type root growth (Fig. 3C). Insensitivity to 24-epibrassinolide is extreme in *ucu1-1/ucu1-1* and *ucu1-2/ucu1-2* roots but only moderate in those of *ucu1-3/ucu1-3* individuals.

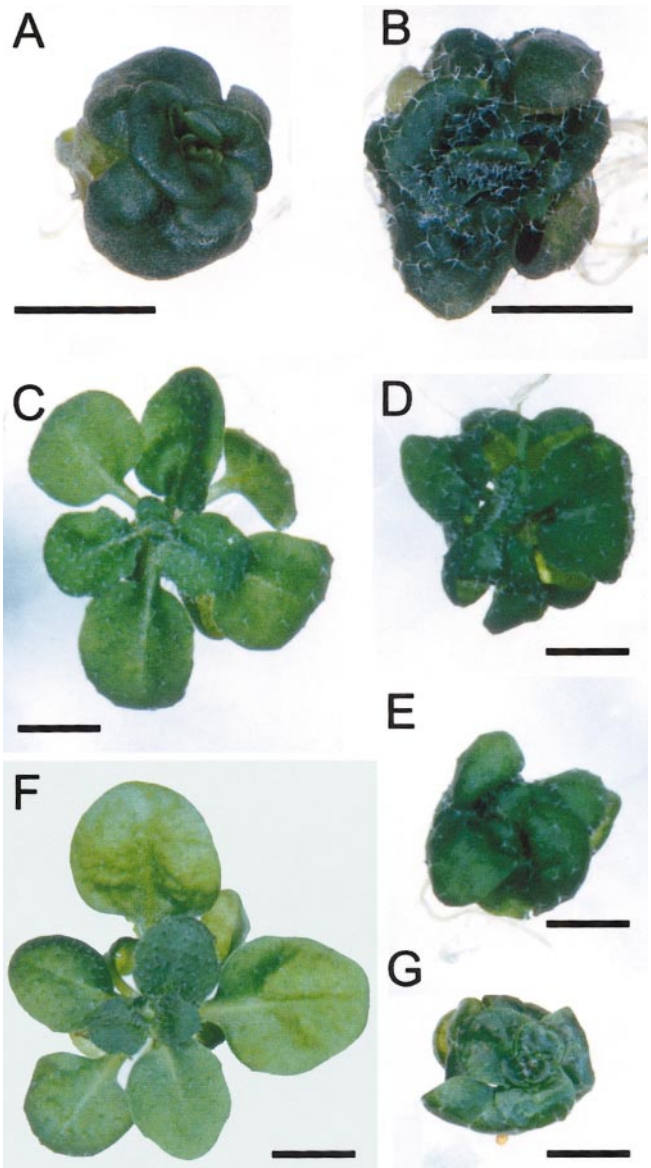

FIG. 4. Genetic interactions between the *UCU1* gene and *BRI1, AXR2,* or *SHY2* genes. (A) *bri1-1/bri1-1,* (B) *bri1-1 ucu1-1/bri1-1 ucu1-1,* (C) *AXR2/axr2-1,* (D) *AXR2/axr2-1;UCU1/ucu1-3,* (E) *AXR2/axr2-1;UCU1/ucu1-1,* (F) *shy2-3/shy2-3,* and (G) *SHY2/shy2-3;UCU1/ucu1-3.* Pictures were taken 23 days after sowing. Scale bars: 2 mm.

The *ucu1* mutants display a wild-type gravitropic response, although a constitutive photomorphogenic response was shown when grown in the dark, a trait that was stronger in *ucu1-1/ucu1-1* and *ucu1-2/ucu1-2* homozygous individuals, which exhibited an extreme de-etiolated phenotype (Fig. 3D), with short hypocotyls and developing true leaves when grown for 21 days in the dark.

Double Mutant Analysis

The overall morphology and the de-etiolated phenotype of *ucu1* mutants, together with their insensitivity to 24-epibrassinolide and hypersensitivity to 2,4-D, suggested that the *UCU1* gene may play a role in the transduction of both auxin and brassinosteroids signals. This prompted us to obtain double mutant combinations in order to detect interactions between *ucu1-1* and mutations affecting responses to auxin [*axr2-1* (*auxin resistant2*; Wilson *et al.*, 1990) and *shy2-3* (*short hypocotyl2*; Tian and Reed, 1999)], brassinosteroid biosynthesis [*det2-1* (*de-etiolated2*; Li *et al.*, 1996) and *dim1-1* (*diminuto1*; Takahashi *et al.*, 1995)], and brassinosteroid perception [*bri1-1* (*brassinosteroid insensitive1*; Clouse *et al.*, 1996)]. Leaf phenotypes were shown to be merely additive in the double mutants involving *det2* and *dim1,* with smaller vegetative leaves than in *ucu1* single mutants, and somewhat curled downward (data not shown). Given that the phenotype of *ucu1 bri1* double mutant plants is extreme (Fig. 4B), it is not easy to discriminate between additivity and epistasis. It must be noted, however, that in the double mutant, both the rosette and the inflorescence are more similar to those of *bri1* than those of *ucu1* single mutants, which suggests an epistatic effect of *BRI1* over *UCU1*.

On the other hand, both *UCU1/ucu1-3;AXR2/axr2-1* (Fig. 4D) and *UCU1/ucu1-1;AXR2/axr2-1* (Fig. 4E) double heterozygotes display a synergistic phenotype that is characterized by a dark green compact rosette and small epinastic leaves, similar to those of brassinosteroid-deficient dwarf mutants. Such a phenotype is stronger in *UCU1/ucu1-1;AXR2/axr2-1* individuals, which were also sterile. Similar results were obtained for *UCU1/ucu1;SHY2/shy2-3* double heterozygotes (Fig. 4G). Hence, in these double heterozygotes, a recessive mutation in the *UCU1* gene, *ucu1-3,* strongly modifies the phenotypes of a completely dominant mutation in the *AXR2* gene, *axr2-1,* or a semidominant mutation in the *SHY2* gene, *shy2-3*. These results clearly indicate a functional relationship between the *UCU1* gene and *AXR2* and *SHY2* genes.

Isolation of the UCU1 Gene

The *UCU1* gene was mapped to chromosome 4 (Fig. 5A), flanked by the *SC5* and *g3883* CAPS (cleaved amplified polymorphic sequences) markers, and tightly linked to the AG CAPS marker (Koniezcny and Ausubel, 1993; http://www.arabidopsis.org/maps/CAPS_Chr4.html). Allelism to the *GIBBERELLIN REQUIRING5* (*GA5*) gene (Koornneef and van der Veen, 1980), whose mutations cause dwarfism and map close to *AG,* was ruled out after the corresponding crosses between *ga5-1* and *ucu1-2* or *ucu1-3* plants. Several new SSLP (simple sequence length polymorphisms; Bell and Ecker, 1994) markers were developed within this region (Fig. 5A), based on the available genomic sequences of BAC (bacterial artificial chromosome) clones (http://mips.gsf.de/proj/thal/), and used to screen for recombinants in an F_2 mapping population of 810 plants. Fine mapping using

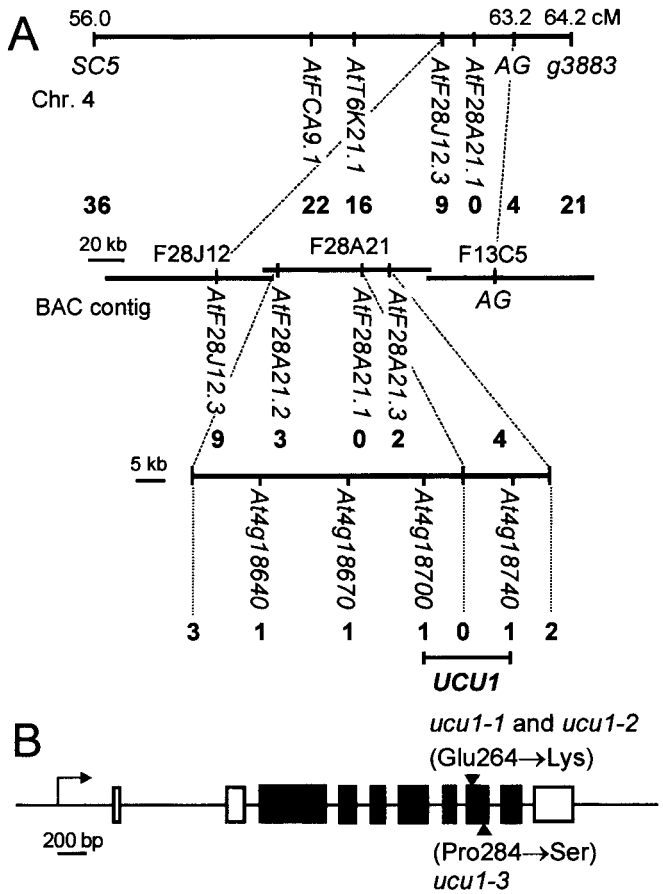

FIG. 5. Positional cloning of the *UCU1* gene. (A) By means of low-resolution mapping, the *UCU1* gene was found to map at chromosome 4, at 6.25 ± 1.27 (n = 370) and 4.50 ± 0.99 cM (n = 446), respectively, from the *SC5* and *g3883* markers. The development of novel SSLP and SNP markers (shown in italics) within this region delimited first the mutation to a region of 80 kb, and finally to a 15-kb interval. The number of recombinant chromosomes found is shown in bold. (B) Structure of the *UCU1* transcription unit and positions of the *ucu1* mutations. Exons are indicated by boxes and introns by lines between boxes. Filled boxes indicate exons encoding the catalytic kinase domain of UCU1.

these new markers delimited the *UCU1* gene to an interval of 80 kb, located within the F28A21 BAC clone (Fig. 5A). The sequencing of several genes contained within F28A21 was instrumental in developing new single nucleotide polymorphism (SNP; Kruglyak, 1997) markers, which enabled us to localize the *UCU1* gene within a region of 15 kb (Fig. 5A). Such a region was fully sequenced in the three *ucu1* mutant lines, allowing us to find point mutations in the coding sequence of an already described gene: *ASKη* (Dornelas *et al.*, 1998). Although isolated from different parental groups, both the *ucu1-1* and *ucu1-2* alleles present a single nucleotide substitution G→A that changes the acidic Glu (E) to basic Lys (K) at amino acid position 264 in a conserved region of the subdomain X of the kinase (as defined by Hanks, 1991), whereas the *ucu1-3* mutation is a C→T substitution that changes the highly conserved Pro (P) to Ser (S) at amino acid position 284 (Figs. 5B and 6). These mutations are likely to damage the three-dimensional structure of a domain that is highly conserved among SGG/GSK3 proteins (Fig. 6) and whose function is unknown. Aiming to determine whether or not *ucu1* mutations modify the expression of the *UCU1* gene, we performed semiquantitative RT-PCR assays, only to find there were no differences related to the wild type in its expression in leaves and flower organs (data not shown).

DISCUSSION

We demonstrate in this work that the *UCU1* gene encodes an AtSK kinase which is involved in the cross-talk between the signaling pathways of brassinosteroids and auxin. Brassinosteroids are essential plant growth regulators similar to animal steroid hormones that participate in diverse developmental programs, including cell expansion, vascular differentiation, etiolation, reproductive development, and stress responses (Bishop and Yokota, 2001). Genetic and molecular analysis of *Arabidopsis thaliana* dwarf mutants have shed light on the biosynthetic pathway of brassinolide, the most active brassinosteroid (Altmann 1999; Bishop and Yokota, 2001; Clouse 1996; Li and Chory, 1999). Attempts to genetically identify components of the brassinosteroid signal transduction pathway have rendered in *A. thaliana* and rice over 20 brassinosteroid insensitive mutants of a single locus, *BRASSINOSTEROID INSENSITIVE1* (*BRI1*), which encodes a leucine-rich repeat (LRR) Ser/Thr kinase that acts as a membrane receptor transducing the signal into the nucleus via protein phosphorylation through a still unclear signaling mechanism (He *et al.*, 2000; Li and Chory, 1997; Wang *et al.*, 2001; Yamamuro *et al.*, 2000). Brassinosteroid-insensitive mutants similar to *bri1* have been found in other plant species, such as *lka* (Nomura *et al.*, 1997) of pea and *curl-3* (Koka *et al.*, 2000) of tomato, which is additionally hypersensitive to 2,4-D, just like the *ucu1* mutants described in this work. Two additional brassinosteroid-insensitive semidominant mutants, named *bin2-1* and *bin2-2*, have been recently reported (Li *et al.*, 2001). Both the phenotype and map position of *bin2* mutations make them likely to be alleles of the *UCU1* gene (Berná *et al.*, 1999).

Although the genome of *A. thaliana* contains about 170 LRR-receptor kinases, only one of them, that of CLAVATA1 (CLV1), has been characterized in detail (Clark, 2001; Fletcher and Meyerowitz, 2000). Activation of the CLV1 signaling pathway is triggered by the interaction between the secreted CLV3 protein and the CLV1 transmembrane LRR receptor kinase complex. The latter includes the CLV1 and CLV2 receptor-like proteins, a kinase-associated protein phosphatase (KAPP), and a Rop GTPase protein among others (Fletcher and Meyerowitz, 2000). It

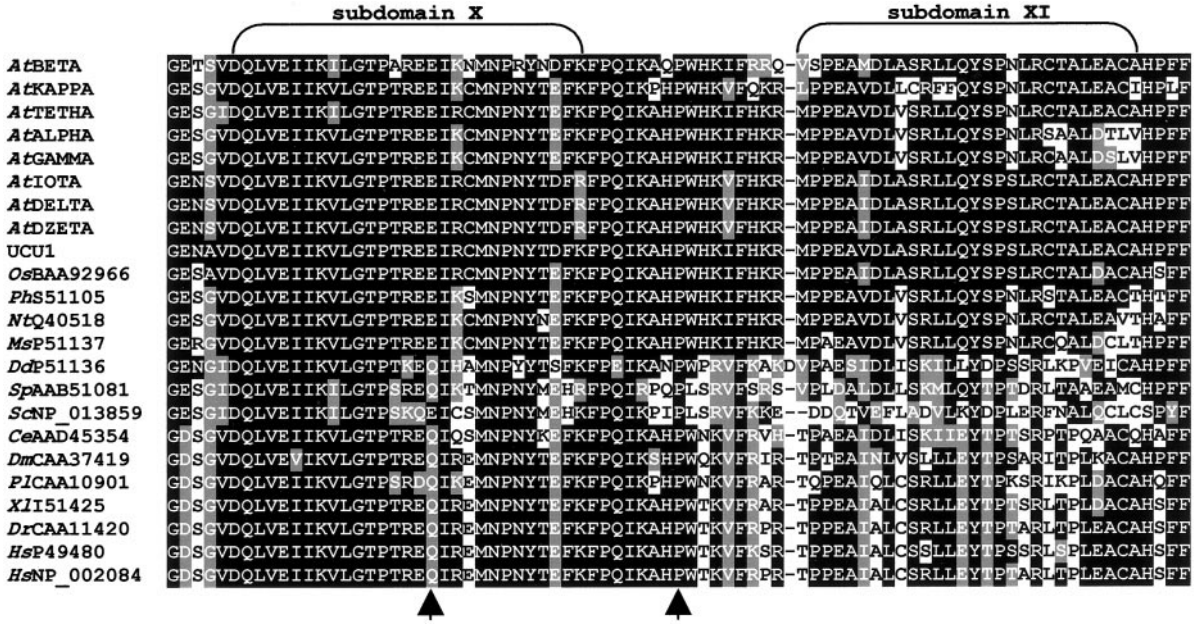

FIG. 6. Alignment of the subdomains X and XI of UCU1 with the corresponding regions of other SGG/GSK3 family members. Arrowheads indicate the amino acids affected by *ucu1* mutations. All the available sequences of UCU1 paralogs are shown, together with those of other SGG/GSK3 family members assumed to be UCU1 orthologs. Amino acids identical to the corresponding residues in the UCU1 sequence are shown in black fields; and similar amino acids are shaded. Names indicate the species and accession numbers of the SGG/GSK3 proteins (*Sc, Saccharomyces cerevisiae; Sp, Schizosaccharomyces pombe; Dd, Dictyostelium discoideum; Ce, Caenorhabditis elegans; Dm, Drosophila melanogaster; Pl, Paracentrotus lividus; Dr, Danio rerio; Xl, Xenopus laevis; At, Arabidopsis thaliana; Os, Oryza sativa; Nt, Nicotiana tabacum; Ms, Medicago sativa; Ph, Petunia hybrida; Hs, Homo sapiens*).

has been described that plants transgenic for antisense constructs of *AtSK11* (*ASKα*) or *AtSK12* (*ASKγ*) display defects in the number of floral organs, primarily due to an increase in meristem size, a phenotype reminiscent to that of the *clv* mutants (Dornelas *et al.*, 2000). Interestingly, transgenic plants carrying a dominant negative GDP-bound form of the Rop2 GTPase (the product of 1 of the 11 Rop GTPase genes found in *A. thaliana*), display small rounded leaves, similar to those of brassinosteroid-deficient mutants, and are, in addition, partially sensitive to brassinosteroid mediated hypocotyl elongation, suggesting a role for Rop GTPases in the regulation of brassinosteroid mediated *Arabidopsis* seedling development (Li *et al.*, 2001). The dwarf phenotype and brassinosteroid insensitivity displayed by *ucu1* mutants, together with the intracellular nature of AtSK proteins, suggest a role for UCU1 as an element acting downstream of BRI1 in the brassinosteroid signaling pathway. This hypothesis is also supported by the apparent epistasis of *BRI1* over *UCU1* as deduced from the phenotype of *ucu1 bri1* double homozygotes. Our data create the possibility that plant SHAGGY/GSK3-related protein kinases, which evolved independently of the Wingless/Wnt pathway, absent in plants, had been recruited to participate in signaling cascades involving LRR receptor kinases.

The *Aux/IAA* gene family members *AXR2* and *SHY2* are assumed to be involved in some early step of an auxin response pathway, participating in a redundant manner in a negative regulatory feedback auxin loop (Nagpal *et al.*, 2000). Both *axr2-1* and *shy2-3* are gain-of-function mutations, which are likely to increase, respectively, the stability of the IAA7 (AXR2) and IAA3 (SHY2) proteins (Ouellet *et al.*, 2001). The synergistic phenotypes of the double heterozygotes of *ucu1* with *axr2* and *shy2* can be explained by assuming that these mutations in *IAA* genes dramatically raise the threshold of *UCU1* activity required for normal plant development. This can be made possible by increasing either the endogenous auxin production or the brassinosteroid insensitivity caused by *ucu1* alleles in a manner which even obliterates the activity of one dose of the wild-type allele of the *UCU1* gene as found in the double heterozygotes involving *ucu1-3*.

The reduction in cell expansion along the proximodistal axis exhibited by most organs of *ucu1* mutants can be explained as a consequence of their insensitivity to brassinosteroids, which, together with auxins, are known to induce the genes for xyloglucan endotransglycosylases, wall-modifying proteins involved in cell expansion (Campbell and Braam, 1999). In addition, brassinosteroids have been shown to promote the orientation of microtubules, that in turn, regulates cell elongation (Mayumi and Shibaoka, 1995) and to rescue the microtubule disorganiza-

tion shown by the *A. thaliana bul1/dwf7/ste1* dwarf mutant affected in brassinosteroid biosynthesis (Catterou *et al.*, 2001). The *det3* cell expansion mutant of *A. thaliana* exhibits a reduced response to brassinosteroids and has been shown to be impaired in the subunit C of the vacuolar H^+-ATPase (V-ATPase), which is, in turn, phosphorylated *in vitro* by BRI1 (Schumacher *et al.*, 1999). Another possibility could be that UCU1 participates in the activation of V-ATPases through BRI1 signaling in brassinosteroid-induced cell elongation.

Contrary to wild-type *A. thaliana* vegetative leaves, which are flattened organs, those of *ultracurvata* mutants are rolled spirally downward. The Ucu1 leaf phenotype is one of the most extreme mutant phenotypes that we have obtained in previous screenings for mutations causing morphological perturbations in the architecture of *Arabidopsis* leaves (Berná *et al.*, 1999; Robles and Micol, 2001). The function of *UCU1* is differentially required in adaxial and abaxial leaf tissues, as deduced from their circinate morphology and a more pronounced misexpansion of abaxial cells.

The phenotypes of homozygous *ucu1* individuals and the hybrid progeny of their intercrosses clearly indicate additive effects of the mutant alleles of the *UCU1* gene studied in this work. These results, taken together with the wild-type phenotype displayed by *UCU1/UCU1/ucu1* triploid plants, can be explained assuming that the recessive allele is hypomorphic and the semidominant alleles antimorphic. Alternatively, the latter might be null or extremely hypomorphic if the *UCU1* gene were haploinsufficient.

The key elements of the patterning mechanisms acting throughout plant development are cell division and cell expansion, together with their coordination and responses to environmental and endogenous signals (Tsiantis and Langdale, 1998). It is now known that complex interactions and cross-talk between signaling pathways of such endogenous signals, plant hormones, control plant development. This is illustrated by the numerous physiological examples of synergy, antagonism, and causal relationship between phytohormones, as well as by pleiotropy in the phenotypes of hormone mutants, some of which display altered responses to more than one hormone (Chory and Wu, 2001). Individual proteins can be responsible for such interconnections among pathways, which become parts of interacting signaling networks (Lu and Fedoroff, 2000; Weng *et al.*, 1999; Weston and Davis, 2001). Given that the *UCU1* gene is likely to be involved in the overlapping of brassinosteroids and auxin signaling pathways, its mutant alleles may help to unravel the complex interactions between plant hormonal pathways. In fact, GSK3 is involved in both Wnt signaling and the specification of cell fates during embryonic development, and also in insulin signaling and metabolic regulation (Weston and Davis, 2001). If such a single kinase transmits signals from multiple receptors in animal cells, its plant counterpart might do so in plant cells, transducing both the brassinosteroids signal and that of auxin.

ACKNOWLEDGMENTS

We thank H. Candela, V. Quesada, P. Robles, and two anonymous referees for comments on the manuscript, and J. M. Serrano and S. Gerber for technical assistance. This research was supported by grants from the Ministerio de Educación y Cultura of Spain (PB95-0685 and PB98-1389). J. M. P-P. was fellow of the Conselleria de Cultura, Educació i Ciència of the Generalitat Valenciana.

REFERENCES

Altmann, T. (1999). Molecular physiology of brassinosteroids revealed by the analysis of mutants. *Planta,* **208,** 1–11.

Altschul, S. F., Gish, W., Miller, W., Myers, E. W., and Lipman, D. J. (1990). Basic local alignment search tool. *J. Mol. Biol.* **215,** 403–410.

Bell, C. J., and Ecker, J. R. (1994). Assignment of 30 microsatellite loci to the linkage map of *Arabidopsis*. *Genomics* **19,** 137–144.

Berná, G., Robles, P., and Micol, J. L. (1999). A mutational analysis of leaf morphogenesis in *Arabidopsis thaliana*. *Genetics* **152,** 729–742.

Bishop, G. J., and Yokota, T. (2001). Plants steroid hormones, brassinosteroids: Current highligths of molecular aspects on their synthesis/metabolism, transport, perception and response. *Plant Cell Physiol.* **42,** 114–120.

Byrne, M., Timmermans, M., Kidner, C., and Martienssen, R. (2001). Development of leaf shape. *Curr. Opin. Plant Biol.* **4,** 38–43.

Campbell, P., and Braam, J. (1999). Xyloglucan endotransglycosylases: Diversity of genes, enzymes and potential wall-modifying functions. *Trends Plant Sci.* **9,** 361–366.

Candela, H., Martínez-Laborda, A., and Micol, J. L. (1999). Venation pattern formation in *Arabidopsis thaliana* vegetative leaves. *Dev. Biol.* **205,** 205–216.

Catterou, M., Dubois, F., Schaller, H., Aubanelle, L., Vilcot, B., Sangwan-Norreel, B. S., and Sangwan, R. S. (2001). Brassinosteroids, microtubules and cell elongation in *Arabidopsis thaliana*. II. Effects of brassinosteroids on microtubules and cell elongation in the *bul1* mutant. *Planta* **212,** 673–683.

Chory, J., and Wu, D. (2001). Weaving the complex web of signal transduction. *Plant Physiol.* **125,** 77–80.

Clark, S. E. (2001). Meristems: Start your signaling. *Curr. Opin. Plant Biol.* **4,** 28–32.

Clouse, S. D. (1996). Molecular genetic studies confirm the role of brassinosteroids in plant growth and development. *Plant J.* **10,** 1–8.

Clouse, S. D., Langford, M., and McMorris, T. C. (1996). A brassinosteroid-insensitive mutant in *Arabidopsis thaliana* exhibits multiple defects in growth and development. *Plant Physiol.* **111,** 671–678.

Dornelas, M. C., Lejeune, B., Dron, M., and Kreis, M. (1998). The *Arabidopsis SHAGGY-related protein kinase (ASK)* gene family: Structure, organization and evolution. *Gene* **212,** 249–257.

Dornelas, M. C., Van Lammeren, A. A., and Kreis, M. (2000). *Arabidopsis thaliana* SHAGGY-related protein kinases (AtSK11

and 12) function in perianth and gynoecium development. *Plant J.* **21,** 419–429.

Dornelas, M. C., Wittich, P., von Recklinghausen, I., van Lammeren, A., and Kreis, M. (1999). Characterization of three novel members of the *Arabidopsis SHAGGY-related protein kinase (ASK)* multigene family. *Plant Mol. Biol.* **39,** 137–147.

Ferkey, D. M., and Kimelman, D. (2000). GSK-3: New thoughts on an old enzyme. *Dev. Biol.* **225,** 471–479.

Fletcher, J. C., and Meyerowitz, E. M. (2000). Cell signaling within the shoot meristem. *Curr. Opin. Plant Biol.* **3,** 23–30.

Hanks, S. K. (1991). Eukaryotic protein kinases. *Curr. Opin. Struct. Biol.* **1,** 369–383.

He, Z., Wang, Z. Y., Li, J., Zhu, Q., Lamb, C., Ronald, P., and Chory, J. (2000). Perception of brassinosteroids by the extracellular domain of the receptor kinase BRI1. *Science* **288,** 2360–2363.

Karsch-Mizrachi, I., and Ouellette, B. F. (2001). The GenBank sequence database. *Methods Biochem. Anal.* **43,** 45–63.

Kim, L., and Kimmel, A. R. (2000). GSK3, a master switch regulating cell-fate specification and tumorigenesis. *Curr. Opin. Genet. Dev.* **10,** 508–514.

Koka, C. V., Cerny, R. E., Gardner, R. G., Noguchi, T., Fujioka, S., Takatsuto, S., Yoshida, S., and Clouse, S. D. (2000). A putative role for the tomato genes *DUMPY* and *CURL-3* in brassinosteroid biosynthesis and response. *Plant Physiol.* **122,** 85–98.

Konieczny, A., and Ausubel, F. M. (1993). A procedure for mapping *Arabidopsis* mutations using co-dominant ecotype-specific PCR-based markers. *Plant J.* **4,** 403–410.

Koornneef, M., and van der Veen, J. H. (1980). Induction and analysis of gibberellin sensitive mutants in *Arabidopsis thaliana* (L.) Heynh. *Theor. Appl. Genet.* **58,** 257–263.

Kosambi, D. D. (1944). The estimation of map distance from recombination values. *Ann. Eugen.* **12,** 172–175.

Kruglyak, L. (1997). The use of a genetic map of biallelic markers in linkage studies. *Nat. Genet.* **17,** 21–24.

Li, H., Shen, J. J., Zheng, Z. L., Lin, Y., and Yang, Z. (2001). The Rop GTPase switch controls multiple developmental processes in *Arabidopsis Plant Physiol.* **126,** 670–684.

Li, J., and Chory, J. (1997). A putative leucine-rich repeat receptor kinase involved in brassinosteroid signal transduction. *Cell* **90,** 929–938.

Li, J., and Chory, J. (1999). Brassinosteroid actions in plants. *J. Exp. Bot.* **50,** 275–282.

Li, J., Nagpal, P., Vitart, V., McMorris, T. C., and Chory, J. (1996). A role for brassinosteroids in light-dependent development of *Arabidopsis. Science* **272,** 398–401.

Li, J., Nam, K. H., Vafeados, D., and Chory, J. (2001). *BIN2,* a new brassinosteroid-insensitive locus in *Arabidopsis. Plant Physiol.* **127,** 14–22.

Lu, C., and Fedoroff, N. (2000). A mutation in the *Arabidopsis HYL1* gene encoding a dsRNA binding protein affects responses to abscisic acid, auxin, and cytokinin. *Plant Cell* **12,** 2351–2366.

Mayumi, K., and Shibaoka, H. (1995). A possible double role for brassinolide in the reorientation of cortical microtubules in the epidermal cell of azuki bean epicotyls. *Plant Cell Physiol* **36,** 173–181.

McCarty, D. R., and Chory, J. (2000). Conservation and innovation in plant signaling pathways. *Cell* **103,** 201–209.

Meinke, D., and Koornneef, M. (1997). Community standards for *Arabidopsis* genetics. *Plant J.* **12,** 247–253.

Nagpal, P., Walker, L. M., Young, J. C., Sonawala, A., Timpte, C., Estelle, M., and Reed, J. W. (2000). *AXR2* encodes a member of the Aux/IAA protein family. *Plant Physiol.* **123,** 563–574.

Nomura, T., Nakayama, M., Reid, J. B., Takeuchi, Y., and Yokota, T. (1997). Blockage of brassinosteroid biosynthesis and sensitivity causes dwarfism in *Pisum sativum. Plant Physiol.* **113,** 31–37.

Ouellet, F., Overvoorde, P. J., and Theologis, A. (2001). IAA17/AXR3. Biochemical insight into an auxin mutant phenotype. *Plant Cell* **13,** 829–842.

Piao, H. L., Pih, K. T., Lim, J. H., Kang, S. G., Jin, J. B., Kim, S, H., and Hwang, I. (1999). An *Arabidopsis GSK3/shaggy-like* gene that complements yeast salt stress-sensitive mutants is induced by NaCl and abscisic acid. *Plant Physiol.* **119,** 1527–1534.

Poethig, R. S. (1997). Leaf morphogenesis in flowering plants. *Plant Cell* **9,** 1077–1087.

Ponce, M. R., Pérez-Pérez, J. M., Piqueras, P., and Micol, J. L. (2000). A multiplex reverse transcriptase-polymerase chain reaction method for fluorescence-based semiautomated detection of gene expression in *Arabidopsis thaliana. Planta* **211,** 606–608.

Ponce, M. R., Quesada, V., and Micol, J. L. (1998). Rapid discrimination of sequences flanking and within T-DNA insertions in the *Arabidopsis* genome. *Plant J.* **14,** 497–501.

Ponce, M. R., Robles, P., and Micol, J. L. (1999). High-throughput genetic mapping in *Arabidopsis thaliana. Mol. Gen. Genet.* **261,** 408–415.

Robles, P., and Micol, J. L. (2001). Genome-wide linkage analysis of *Arabidopsis* genes required for leaf development. *Mol. Genet. Genomics* **266,** 12–19.

Scanlon, M. J. (2000). Developmental complexities of simple leaves. *Curr. Opin. Plant Biol.* **3,** 31–36.

Schumacher, K., Vafeados, D., McCarthy, M., Sze, H., Wilkins, T., and Chory, J. (1999). The *Arabidopsis det3* mutant reveals a central role for the vacuolar H(+)-ATPase in plant growth and development. *Genes Dev.* **13,** 3259–3270.

Serrano-Cartagena, J., Candela, H., Robles, P., Ponce, M. R., Pérez-Pérez, J. M., Piqueras, P., and Micol, J. L. (2000). Genetic analysis of *incurvata* mutants reveals three independent genetic operations at work in *Arabidopsis* leaf morphogenesis. *Genetics* **156,** 1363–1377.

Serrano-Cartagena, J., Robles, P., Ponce, M. R., and Micol, J. L. (1999). Genetic analysis of leaf form mutants from the *Arabidopsis* Information Service collection. *Mol. Gen. Genet.* **261,** 725–739.

Siegfried, E., Perkins, L. A., Capaci, T. M., and Perrimon, N. (1990). Putative protein kinase product of the *Drosophila* segment-polarity gene *zeste-white3. Nature* **345,** 825–829.

Sinha, N., Hake, S., and Freeling, M. (1993). Genetic and molecular analysis of leaf development. *Curr. Top. Dev. Biol.* **28,** 47–80.

Takahashi, T., Gasch, A., Nishizawa, N., and Chua, N. H. (1995). The *DIMINUTO* gene of *Arabidopsis* is involved in regulating cell elongation. *Genes Dev.* **9,** 97–107.

The *Arabidopsis* Initiative (2000). Analysis of the genome sequence of the flowering plant *Arabidopsis thaliana. Nature,* **408,** 796–815.

Thompson, J. D., Gibson, T. J., Plewniak, F., Jeanmougin, F., and Higgins, D. G. (1997). The CLUSTAL_X windows interface: Flexible strategies for multiple sequence alignment aided by quality analysis tools. *Nucleic Acids Res.* **25,** 4876–4882.

Tian, Q., and Reed, J. W. (1999). Control of auxin-regulated root development by the *Arabidopsis thaliana SHY2/IAA3* gene. *Development* **126,** 711–721.

Tichtinsky, G., Tavares, R., Takvorian, A., Schwebel-Dugue, N., Twell, D., and Kreis, M. (1998). An evolutionary conserved group of plant GSK-3/shaggy-like protein kinase genes preferentially expressed in developing pollen. *Biochim. Biophys. Acta* **1442,** 261–273.

Tsiantis, M., and Langdale, J. (1998). The formation of leaves. *Curr. Opin. Plant Biol.* **1,** 43–48.

Wang, Z. Y., Seto, H., Fujioka, S., Yoshida, S., and Chory, J. (2001). BRI1 is a critical component of a plasma-membrane receptor for plant steroids. *Nature* **410,** 380–383.

Weng, G., Bhalla, U. S., and Iyengar, R. (1999). Complexity in biological signaling systems. *Science* **284,** 92–96.

Weston, C. R., and Davis, R. J. (2001). Signal transduction: Signaling specificity—a complex affair. *Science* **292,** 2439–2440.

Wigge, P. A., and Weigel, D. (2001). *Arabidopsis* genome: Life without notch. *Curr. Biol.* **11,** R112–R114.

Wilson, A. K., Pickett, F. B., Turner, J. C., and Estelle, M. (1990). A dominant mutation in *Arabidopsis* confers resistance to auxin ethylene and abscisic acid. *Mol. Gen. Genet.* **222,** 377–383.

Woodgett, J. R. (1990). Molecular cloning and expression of *glycogen synthase kinase-3/factor A. EMBO J.* **9,** 2431–2438.

Yamamuro, C., Ihara, Y., Wu, X., Noguchi, T., Fujioka, S., Takatsuto, S., Ashikari, M., Kitano, H., and Matsuoka, M. (2000). Loss of function of a rice *brassinosteroid insensitive1* homolog prevents internode elongation and bending of the lamina joint. *Plant Cell* **12,** 1591–1606.

Received for publication October 18, 2001
Revised November 16, 2001
Accepted November 16, 2001
Published online January 15, 2002